A Hybrid Approach for Optimal Sizing of Inverter-Based Distributed Generation Unit in Presence of Harmonic Distortion Limit

Barnali Motling, Subrata Paul, and Sunita Halder nee Dey

***Abstract*—This paper presents a hybrid approach to calculate the optimal size of inverter-based distributed generation unit located at any given bus of a radial distribution network to minimize the active power loss in the network in presence of limit imposed on the maximum allowable value of total harmonic distortion in bus voltages. The suggested approach combines efficient iterative computations with a rule base developed in the present work, and requires much less computation compared to the evolutionary population based methods reported so far, to reach the desired solution. In support of this claim, the proposed methodology was tested on two bench-mark distribution test systems, and the test results were compared and validated with those obtained using Particle Swarm Optimization technique. PSO has been chosen for comparison as it is one of the most widely used among the evolutionary population based methods due to its simple approach, ease of implementation, and also because of its superiority in terms of precision, robustness and speed of convergence. From the comparative results it has been established that the proposed method can provide solution for the problem undertaken in this work with significantly less computation than is required by the evolutionary computation based methods.**

***Index Terms*—Harmonic distortion limit inverter-based DG unit, network loss minimization, total harmonic distortion, rule base.**

I. Introduction

Integration of distributed generation (DG) in distribution system can provide a number of technical, environmental and economic benefits [1], [2]. But proper planning for optimal DG location and size is required to achieve those benefits to the fullest extent. Reduction in network power loss is one of the most prominent and desirable among those benefits.

Majority of the DG units now-a-days use renewable energy sources. These renewable energy based DG units use power electronic inverters for their interface with the network. Proliferation of these inverter-based DG units along with different types of nonlinear loads has resulted in harmonic distortions in either or both current and voltages in distribution networks. These distortions in currents and voltages have adverse effects on system operation, protection, stability and reliability issues [3]-[5]. It is, therefore, necessary to keep these distortions within some acceptable range to avoid any mal-operation of the system. Such requirements impose the necessity of taking into consideration the effect of harmonics injected by these DG units while solving the problem of optimal planning for their installation.

Consideration of harmonic distortion limit in optimal DG planning for loss minimization in distribution network can be found in the references [6]-[15]. All these authors have used evolutionary population based iterative techniques to solve the optimization problems in their studies. While authors of [6] have used Evolutionary Programming (EP), authors of [7], [8] have applied Genetic Algorithm (GA) to solve the problem. Application of Harmony Search Algorithm (HSA) can be found in the work reported by the authors of [9]. Authors of [10] have employed, Biogeography Based Optimization algorithm (BBO) for the solution of the problem. Particle Swarm Optimization (PSO) has been applied by the authors of [11]-[15] to solve the problem of optimal DG planning in presence of harmonic distortion limit. The aforementioned evolutionary computation based methods have their relative merits and demerits but all of them suffer from a common draw-back. All these methods are computationally highly demanding for optimal DG planning problem as each of them requires large number of harmonic load flow (HLF) calculations [16]-[18] to generate acceptable solution.

In the present study, a hybrid method is proposed for optimal sizing of inverter-based DG unit located at any given bus of a radial distribution network. The method utilizes a computationally efficient iterative technique [19] in combination with a rule base that has been developed in the present study. The solution gives the size of the DG unit that minimizes the network power loss while satisfying the constraint imposed on the allowable limit of THD_{VM} , the maximum total harmonic distortion in bus voltages. The proposed method requires only few HLF to be executed to arrive at an acceptable solution for any given bus, and thus, requires significantly less computation compared to the evolutionary population based methods. To validate this claim, the results obtained using the suggested method has been benchmarked with those obtained using PSO [20]. PSO has been chosen as it is one of the most widely used among the evolutionary population based methods due to its simple approach, ease of implementation, and its superiority [21] over most of the other methods of this category in terms of precision, robustness and speed of convergence.

This paper is organized in the following manner. The problem statement is given in Section II while Section III

Manuscript received December 22, 2021; revised April 20, 2022. This work is a part of research work and is being carried out at Electrical Engineering Department, Jadavpur University, Kolkata, India.

Barnali Motling is with the Electrical Engineering Department, Jadavpur University under QIP Scheme of Government of India, India (e-mail: bsmotling@gmail.com)

Subrata Paul and Sunita Halder nee Dey are with Jadavpur University, Kolkata, India (e-mail: speejupow@yahoo.co.in, sunitaju@yahoo.com).

doi: 10.18178/jocet.2022.10.2.532

elaborates the development of the rule base. Section IV explains the methodology and presents the necessary computational flowchart. Section V presents the results obtained for two benchmark distribution networks, and Section VI draws the conclusion from the present work. Computations required to determine various quantities necessary for execution of the rule base are furnished in Appendices A, B and C. Appendix-D provides the harmonic data used in the present work.

II. PROBLEM STATEMENT

The problem undertaken in the proposed work is to determine the optimal size of inverter-based DG unit located at any given bus of a radial distribution network to achieve maximum possible reduction in network power loss within the allowable limit on THD_{VM}.

The total active power loss in the network including the losses due to harmonics can be expressed as

$$P_{LOSS} = \sum_{h=1}^{\infty} \sum_{m=1}^{B} \left(\left| I_m^h \right|^2 R_m \right) \tag{1}$$

where, B *is* the total number of branches in the network, I_m^h is the *r. m. s.* value of the h-th harmonic component of current through the m-th branch, and R_m is the resistance of the m-th branch.

$$THD_{VM} = \max_i \left(THD_{vi} \right) \tag{2}$$

THD_{vi} is the total harmonic distortion of the i-th bus voltage, and is given by

$$THD_{vi}(\%) = \left(\sqrt{\sum_{h=2}^{\infty} \left| V_i^h \right|^2} \Big/ \left| V_i^1 \right| \right) \times 100$$

where, $i =$ 1,2,3,….n ; n being the number of buses in the network, V_i^1 and V_i^h are, respectively, the r.m.s. values of the fundamental and the h-th harmonic component of the i-th bus voltage. I_m^h, R_m^h, V_i^1 and V_i^h, required in (1) and (2) for calculation of P_{LOSS} and THD_{vi} are obtained from HLF solution.

The problem is posed as an optimization problem. The objective function to be minimized is given by equation (1). The equality constraint is given by the following real power balance equation

$$P_{ss} + P_g = \sum_{i=1}^{N} P_{L_i} + P_{LOSS} \tag{3}$$

where, $P_{ss} =$ real power fed by the substation

$P_g =$ real power generated by the DG

$P_{L_i} =$ real power demand by the load at i^{th} bus

whereas, the inequality constraints are given by

$$P_{g_{\min}} \le P_g \le P_{g_{\max}} \tag{4}$$

and $$THD_{VM} \le THD_L \tag{5}$$

where, $P_{g_{\min}}$ and $P_{g_{\max}}$ are minimum and maximum limits of DG active power output and THD_L represents the specified limit on the maximum allowable value of THD_{VM}.

III. DEVELOPMENT OF THE RULE BASE

In the present work, the rule base is developed from the following observations:

A. Observation 1

An extensive simulation study was done for a number of radial distribution network using repeated HLF calculations. For each network, the study was carried out by running HLF with the DG unit placed at different buses, taken one at a time, and the DG size varied in small steps. In each case, P_{LOSS} and THD_{VM} were calculated from the HLF result. The HLF method presented in [16] has been used in the present study. From the results, it was revealed that, with increase in size of the DG source placed at any given bus of a radial distribution network, the value of THD_{VM} may vary in one of the following manner:

(i) With background harmonics present in the network the value of THD_{VM} starts decreasing from THD_B (the background value of THD_{VM}), and, after attaining a minimum, starts to increase monotonically. In some cases, THD_{VM} may increase monotonically starting from THD_B.

(ii) With no background harmonics present, the value of THD_{VM} increases monotonically from zero (as $THD_B = 0$).

The variation of THD_{VM} with DG size, henceforth, will be termed as THD curve. The above mentioned nature of THD curve can be explained as follows:

The initial decreasing nature of the THD curve is due to possible cancellation of some of the background harmonics by the DG injected harmonics. As the DG size increases, resultant magnitude of those common harmonics go on reducing causing the value of THD_{VM} to go down gradually. This trend continues up to a DG size for which the cancellation is complete, and after that, the magnitude of those common harmonics starts to increase with the DG size resulting in an increasing trend in the THD curve. However, depending on the background harmonic profile and the profile of the DG injected harmonics, the cancellation may not be appreciable or no cancellation may occur at all. In that case, the THD curve increases monotonically starting from THD_B If $THD_B = 0$, the THD curve increases monotonically from zero as there is only DG injected harmonics which only increases with DG size.

Fig. 1(a) and Fig. 1 (b) show the THD curves for some of the buses of IEEE-33 bus network [22] and IEEE-69 bus network [23] respectively with the load data for both the systems modified by loading condition L2 as mentioned in Table D1 of Appendix-D to incorporate the effects of harmonics due to nonlinear loads. To maintain clarity of these figures, curves for only a few arbitrarily selected buses have been shown.

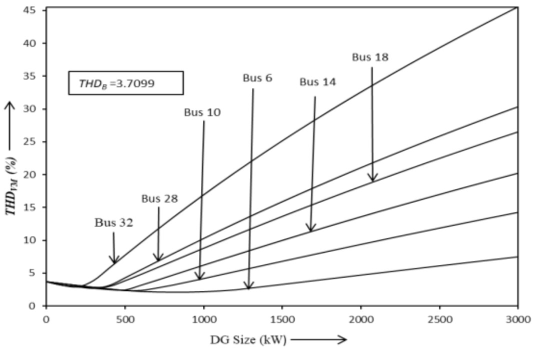

(a)

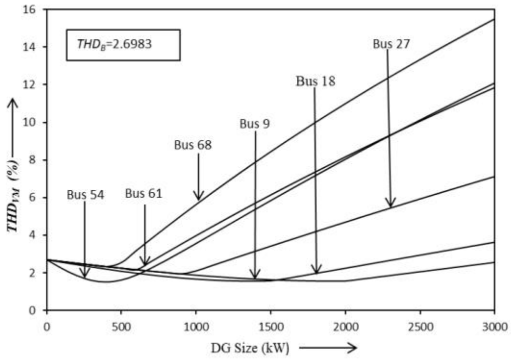

(b)

Fig. 1. (a). THD curves for different buses of IEEE-33 bus network under loading condition L2 (b). THD curves for different buses of IEEE-69 bus network under loading condition L2

To demonstrate the effect of base case loading on the *THD* curves, the same for bus 12 of IEEE 33 bus network with different degrees of nonlinearities in the base case loading (as given by different loading conditions L1, L2, and L3) have been presented in Fig. 2

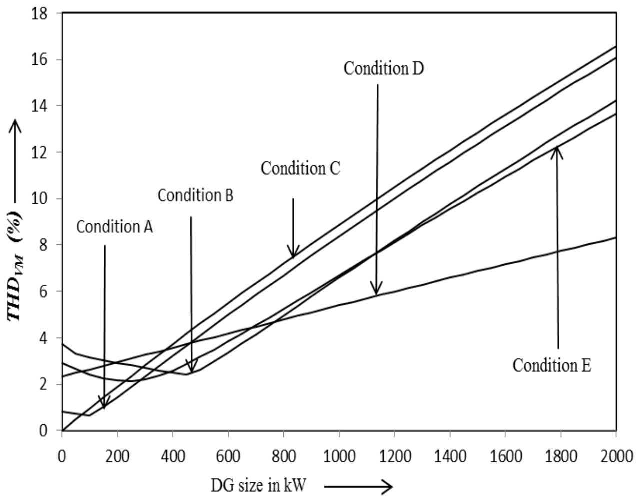

Fig. 2. THD curves for Bus 12 of IEEE-33 network under various conditions.
A: Under loading condition L1 ($THD_{B=}$ 0.8126)
B: Under loading condition L2 ($THDB_=$ 3.7099)
C: Under loading condition L3 ($THDB_=$ 0)
D: Under loading condition L1 with 300kW DG placed at Bus 26 ($THD_{B=}$ 2.33086)
E: Under loading condition L2 with 200kW DG placed at Bus 30 ($THD_{B=}$ 2.92546).

B. Observation 2

A typical *THD* curve is shown in Fig. 3. S_{L1} and S_{L2} are the sizes for which $THD_{VM} = THD_L$. THD_m represents the minimum value of THD_{VM} within the range of DG size considered, and S_m is the corresponding size of the DG. S_{Max} and S_{Min} are, respectively, the maximum and minimum DG sizes considered, and THD_{Max} and THD_{Min} are the corresponding values of THD_{VM}. It is obvious from this figure that, within the range of DG size considered, a *THD* curve can intersect the THD_L line at the most for two sizes, once at S_{L1} in the decreasing zone of the *THD* curve, and, for the second time, at S_{L2} (with $S_{L2} > S_{L1}$) in the increasing zone. A decrement in size from S_{L1} will raise the value of THD_{VM} above THD_L while the same will take place for an increment in size from S_{L2} which means S_{L1} and S_{L2} are the limiting sizes as far as the constraint on maximum limit of THD_{VM} is concerned. For any size S, where $S_{L1} < S < S_{L2}$, the value of THD_{VM} will be within THD_L. This can happen only if $THD_{Min} > THD_L < THD_{Max}$ with $THD_m < THD_L$. However if $THD_{Min} < THD_L < THD_{Max}$, then, S_{L2} will be the only intersecting point. In that case, THD_{VM} will be within limit only for sizes smaller or same as S_{L2}. On the other hand, if $THD_{Min} > THD_L > THD_{Max}$, S_{L1}, will be the only intersecting point and THD_{VM} will be within limit only for sizes larger than or equal to S_{L1}, When both THD_{Max} and THD_{Min} are less than THD_L, for all the sizes within the range, THD_{VM} will be within the limit. In case $THD_{Min} = THD_L$, S_{L1} coincides with S_{Min}, while S_{L2} coincides with S_{Max} when $THD_{Max} = THD_L$. No size will be available for which $THD_{VM} \le THD_L$ if $THD_{VM} > THD_L$.

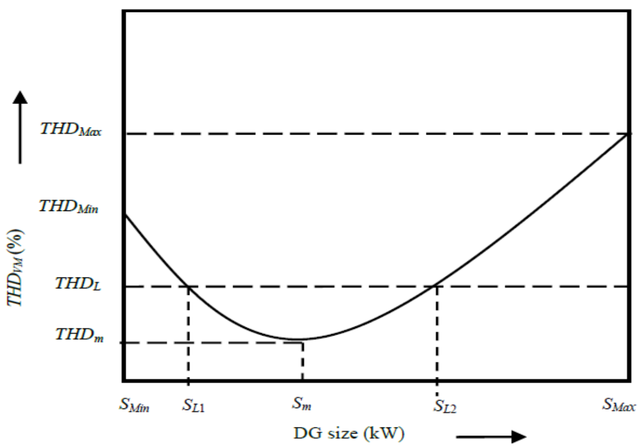

Fig. 3. A typical THD curve.

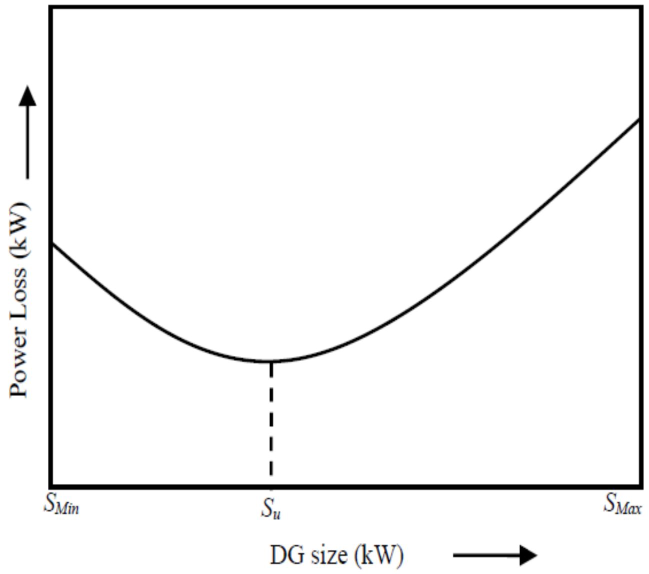

Fig. 4. A typical loss curve.

C. Observation 3:

It has been shown in [24] that the network power loss varies in a parabolic pattern with the DG size at any given bus of a radial distribution network when no harmonics are present in the network. An earlier study [19] demonstrated in presence of DG injected harmonics, shows that the variation of network power loss with the size of DG source placed at any given bus has almost same nature as that taking place in absence of any harmonics present in the network. Fig. 4 shows a typical loss curve, where S_u is the unconstrained optimal size of the DG, i.e., the size that minimizes the network power loss with no constraint imposed on the maximum allowable value of THD_{VM} .Based on the above observations, a rule base has been developed which can identify the optimal solution S_{opt} under different situations. The rule base has been presented along with all the necessary justifications for each situations in Table I.

TABLE I: THE RULE BASE

Rule	Situations	Optimal solution S_{opt}	Justifications
1	$THD_{Min} < THD_L > THD_{Max}$	$S_{opt} = S_u$	The THD curve lies below the THD_L line for the entire range of DG sizes considered. Hence, no restriction on the optimal size is imposed by THD_L .
2	$THD_{Min} < THD_L < THD_{Max}$	a) $S_{opt} = S_{L2}$ if $S_{L2} < S_u$. b) $S_{opt} = S_u$ if $S_{L2} \geq S_u$.	S_{L2} is the determining factor as the THD curve intersects the THD_L line only once at the size S_{L2}.
3	$THD_{Min} = THD_L < THD_{Max}$	a) If $THD_m < THD_L$, then i) $S_{opt} = S_{L2}$ if $S_{L2} < S_u$. ii) $S_{opt} = S_u$ if $S_{L2} \geq S_u$. b) $S_{opt} = S_{Min}$ if $THD_m = THD_L$.	S_{L1} will coincide with S_{Min}, hence, S_{L2} will be the determining factor. S_{Min} is the only possible solution.
4	$THD_{Min} > THD_L > THD_{Max}$	a) $S_{opt} = S_{L1}$ if $S_{L1} > S_u$ b) $S_{opt} = S_u$ if $S_{L1} \leq S_u$.	S_{L1} is the determining factor as the THD curve intersects the THD_L line only once at the size S_{L1}.
5	$THD_{Min} > THD_L = THD_{Max}$	a) If $THD_m < THD_L$, then i) $S_{opt} = S_{L1}$ if $S_{L1} > S_u$ ii) $S_{opt} = S_u$ if $S_{L1} \leq S_u$.	Both S_{L1} and S_{L2} will exist. S_{L2} will coincide with S_{Max}, so S_{L1} will be the determining factor.
6	$THD_{Min} > THD_L < THD_{Max}$	a) No solution exists if $THD_m > THD_L$ b) $S_{opt} = S_m$ if $THD_m = THD_L$ c) If $THD_m < THD_L$, The possible solutions are as follows : i) $S_{opt} = S_{L2}$, if $S_{L2} \leq S_u$ ii) $S_{opt} = S_{L1}$, if $S_{L1} \geq S_u$ iii) $S_{opt} = S_u$, if $S_{L1} < S_u < S_{L2}$	The THD curve lies above the THD_L line for the entire range of DG size considered. S_m is the only possible solution. The THD curve will intersect the THD_L line at both the sizes S_{L1} and S_{L2}. Therefore, i) Between S_{L1} and S_{L2}, the later size is nearer to S_u, and hence, results in less amount of loss. ii) Between S_{L1} and S_{L2}, the former size is nearer to S_u, and hence, results in less amount of loss. iii) For the entire range of DG size from S_{L1} to S_{L2}, the THD curve lies below the THD_L line.

IV. The Proposed Methodology

The proposed methodology is depicted in the form of a flow chart as shown in Fig.5. The-methodology is pivoted on the rule base developed in section III, and on determination of appropriate quantities determined from the following such as $S_u, THD_u, S_m, THD_m, THD_{Min}$, THD_{Max}, S_{L1} and S_{L2} depending on the rule to be fired. THD_{Min} and THD_{Max} are also necessary for the rule base to select the rule to fire and can be obtained from HLF with DG size S_{Min} and S_{Max} placed one at a time at the selected bus. The computations necessary for determination of other quantities are discussed in appendices.

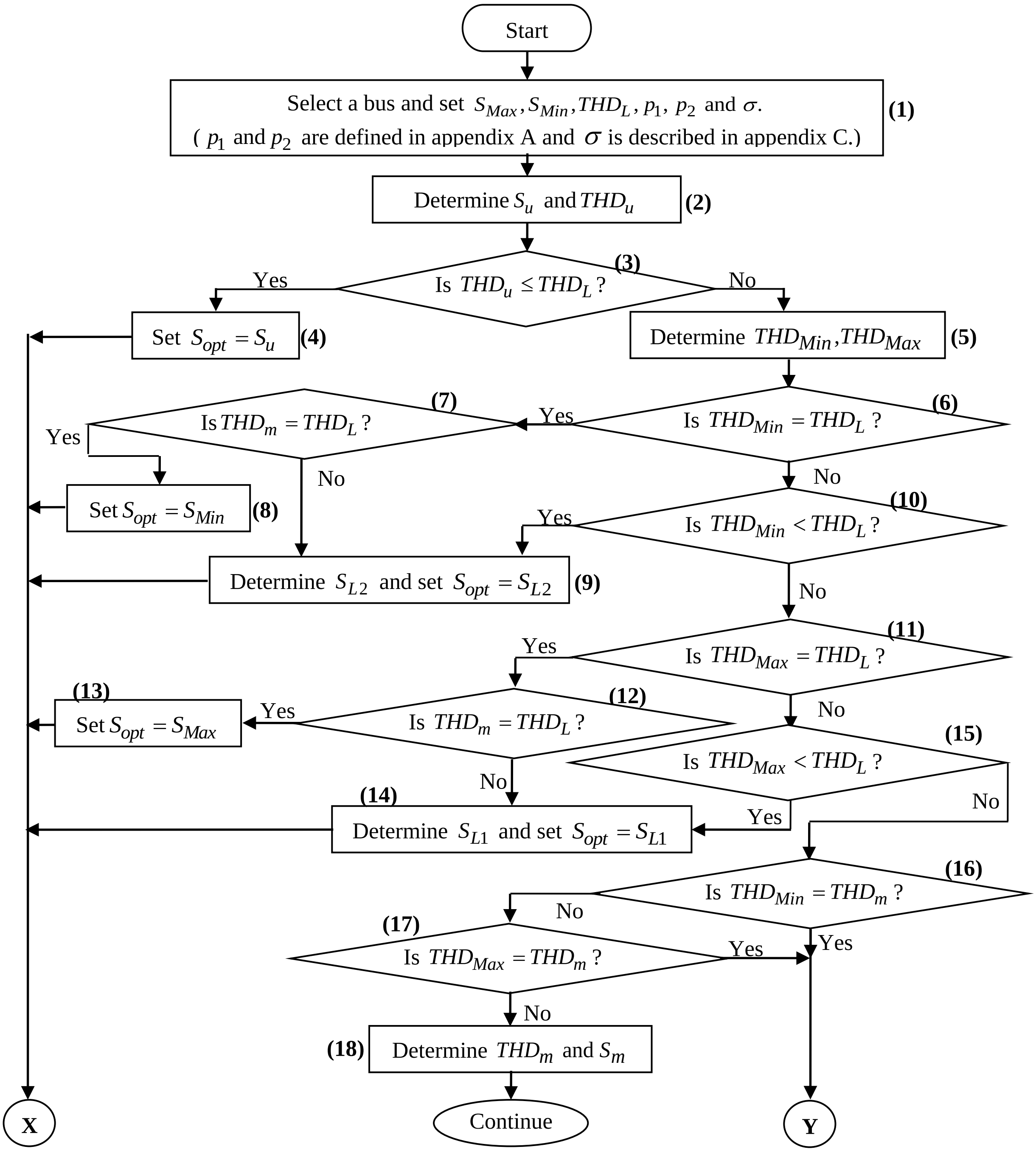

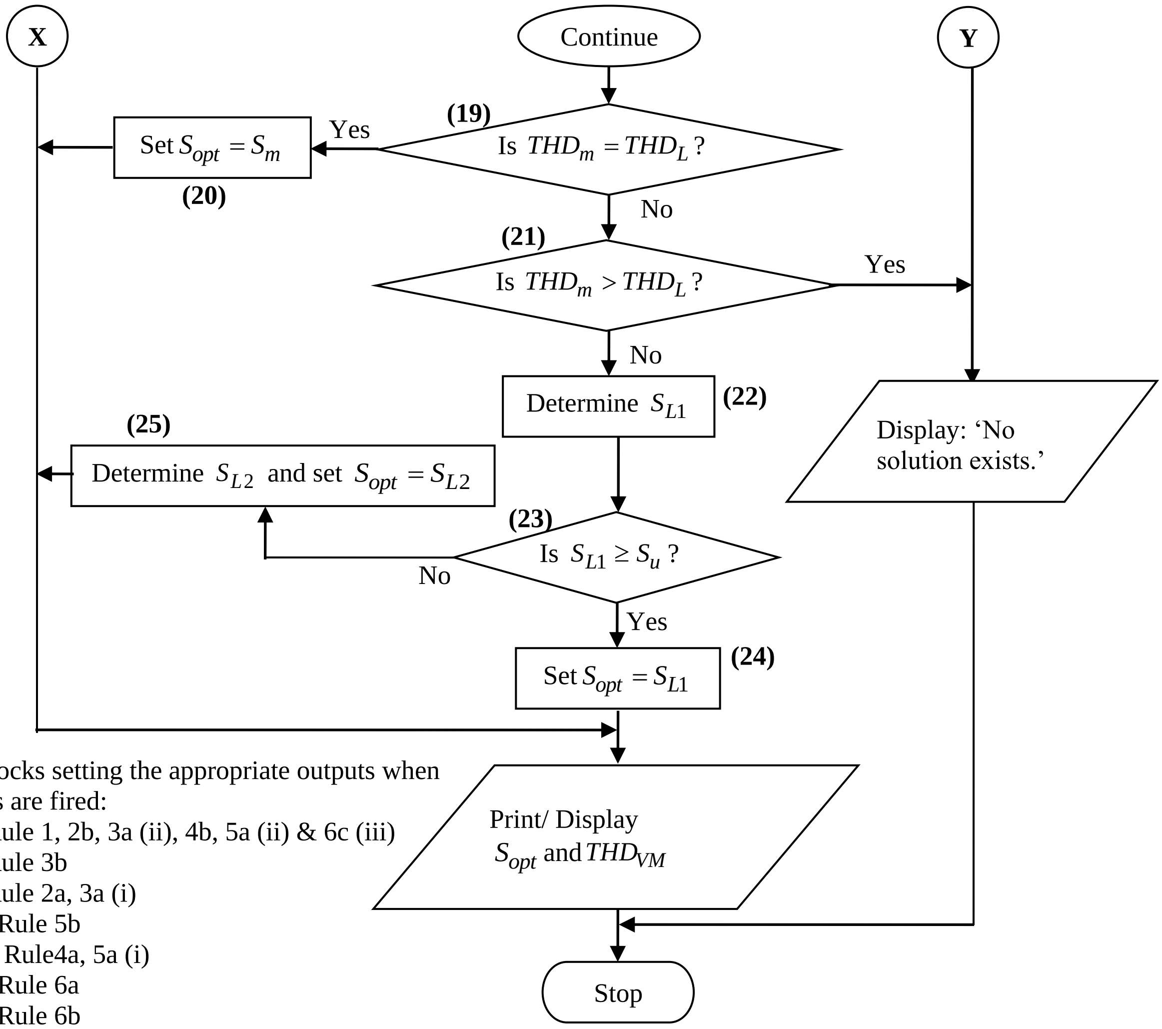

List of the blocks setting the appropriate outputs when relevant rules are fired:

1. Block 4: Rule 1, 2b, 3a (ii), 4b, 5a (ii) & 6c (iii)
2. Block 8: Rule 3b
3. Block 9: Rule 2a, 3a (i)
4. Block 13: Rule 5b
5. Block 14: Rule4a, 5a (i)
6. Block 26: Rule 6a
7. Block 20: Rule 6b
8. Block 24: Rule 6c (ii)
9. Block 25: Rule 6c (i)

Fig. 5. Computational Flowchart.

The following is to be noted in the context of the flowchart:

1) The condition $THD_u \leq THD_L$ is met under all of the situations leading to execution of any of the rules - 1, 2b, 3a (ii), 4b, 5a (ii) and 6c (iii) and all these rules generate same output. Hence, block 3 has been used as the first decision block in the lowchart to derive the following advantages:
   i) The number of decision blocks is reduced as multiple rules are taken care of by this single block.
   ii) No other quantities except S_u and THD_u are required to be determined to fire the appropriate rule in the above-mentioned situations. Hence, computations required under such situations will be minimum.
2) The comparison tasks done in the decision blocks 7, 12, 16 and 17 do not require determination of the value of THD_m. The value of THD_m is required only by the decision blocks 19 and 21. The reason has been explained in details in Appendix B.

V. Results and Discussions

Efficacy of the proposed approach was tested on two benchmark radial distribution test networks, namely, IEEE-33 bus network [22] and IEEE-69 bus network [23]. The load data for the two systems were modified as given in Table D1 of Appendix-D to introduce different degrees of nonlinearity in the load. A combination of different types of nonlinear loads were considered, and the harmonic spectrum [25], [26] of these loads are given in Table D2 to Table D4 of Appendix-D. The DG is assumed to be interfaced with the network through a six pulse converter whose harmonic spectrum [26] is shown in Table D2. For the 33 bus network, bus nos. 6 to 18 from the main trunk and bus nos. 26 to 33 from the longest lateral were chosen for this study, while bus nos. 6 to 27 from the main trunk and bus nos. 53 to 65 from the longest lateral are chosen for the 69 bus network. Only inverter-based DG is of concern in this work. Such DG units operate at unity power factor because of their design [12], hence, unity power factor DG has been considered in this study. Following the recommendation in IEEE-519 [27] a limit of 5% has been imposed on the maximum allowable value of THD_{VM} for both the networks, which means that, the value of THD_L is taken as 5% for this study. The minimum and maximum limit on the size of DG unit to be installed has been considered to be 400 kW and 3000kW respectively. The solutions are obtained with $p_1 = 5,\ p_2 = 0.5$ and $\sigma = 0.001$. p_1, p_2 are defined in Appendix- A and σ is defined in Appendix-C. The results thus obtained with the proposed method have been compared with that obtained using PSO. The comparative results are summarized in Table III (A) to Table IV (C). Table III (A) to Table III (C) show the results for IEEE-33 bus network under loading conditions L1, L2 and L3 respectively. Results for IEEE-69 bus network are shown in Table IV (A) to Table IV (C). For brevity, results of alternate candidate buses are shown for the 69 bus network. The power losses in the two networks prior to installation of the DG are given in Table II.

TABLE II: NETWORK POWER LOSS PRIOR TO INSTALLATION OF THE DG

Network	Power loss (kW)		
	Loading condition L1	Loading condition L2	Loading condition L3
IEEE-33 bus	194. 847	196.18	194.23
IEEE-69 bus	215.235	218.104	215. 0842

From Table III(A), III(B) and III(C), it is found that, under all loading conditions, the unconstrained optimum size for all buses considered in this study violate the constraint on THD_L From the results it is clear that the constrained optimal sizes obtained by the proposed method corroborate with those obtained by PSO. Number of HLF required by the proposed method for each bus is also shown from which it is found that the maximum number of HLF required by the proposed method is 33 which is significantly less than that usually required by PSO in such problems. The PSO formulation used in [15] has been applied in this work taking a swarm size of 10 particles with each particle represented by one DG size. Minimum number of iterations required to get the desired solution by PSO has been found to be 52 for bus 27 under loading condition L1. This means a total of (52x10) =520 number of HLF as one HLF is required for each particle in an iteration. For bus 15 to bus 18 in Table III (A), for bus 17 and bus 18 in Table III (B), and for bus 14 to bus18 and bus 33 in Table III(C), no solution is obtained as, in each case, the value of THD_m, within the range of DG size considered, is found to be above THD_L.

The above results also show appreciable reduction in power loss in all cases where constrained solution is available. From Table IV (A) it is found that, for the IEEE-69 bus system, the constraint on THD_{VM} is not violated for any of the buses of the main trunk, and hence, the constrained sizes for these buses coincide with the unconstrained optimal sizes.

TABLE III (A): OPTIMUM DG SIZES FOR IEEE-33 BUS NETWORK UNDER LOADING CONDITION L1

Bus no.	Without Constraint (By PSO)			With Constraint						
				By proposed iterative approach				By PSO		
	Size (kW)	P_{LOSS} (kW)	THD_{VM} (%)	Size (kW)	P_{LOSS} (kW)	THD_{VM} (%)	No. of HLF reqd.	Size (kW)	P_{LOSS} (kW)	THD_{VM} (%)
6	2376	106.1706	6.937	1716	112.6100	4.9979	18	1718	112.3510	4.9988
7	2255	107.011	9.604	1188	125.6943	4.9959	28	1188	125.6943	4.9959
8	1926	111.1225	9.1265	1064	126.9385	4.9969	29	1064	126.9385	4.9969
9	1600	116.9935	10.1162	795	135.5258	4.9970	30	795	135.5258	4.9970
10	1385	120.5415	10.9531	633	141.2165	4.9941	25	633	141.2165	4.9941
11	1356	121.1517	10.9044	622	141.4375	4.9937	26	622	141.4375	4.9937
12	1298	122.4193	10.7862	601	142.0186	4.9916	30	601	142.0186	4.9916
13	1111	126.9396	11.9894	461	148.8637	4.9942	32	461	148.8637	4.9942
14	1050	128.5122	12.9617	402	152.5371	4.9892	24	405	151.2311	4.9999
15	1000	130.8447	13.4695							
16	940	133.8587	13.7504	No solution is obtained within the range of DG size considered						
17	835	139.0413	15.3375							
18	785	141.8171	15.3868							
26	2248	107.8206	7.058	1595	114.7235	4.9982	27	1595	114.72348	4.9982
27	1968	110.2001	6.7918	1451	117. 4451	4.9974	28	1451	117.44506	4.9974
28	1703	114.7254	9.34	908	131.1808	4.9968	15	908	131.18083	4.9968
29	1513	116.6372	10.6234	706	137.6629	4.9962	27	707	137.13217	4.9995
30	1418	118.265	10.7486	653	139.2393	4.9995	32	653	139.23926	4.9995
31	1245	123.5445	12.0524	509	147.0185	4.9958	33	510	147.00012	4.9995
32	1192	125.6125	12.4852	470	149.6146	4.9953	29	469	149.39324	4.9992
33	1132	128.8873	13.1762	423	153.3416	4.9996	29	423	153.34165	4.9996

TABLE III(B): OPTIMUM DG SIZES FOR IEEE-33 BUS NETWORK UNDER LOADING CONDITION L2

Bus no.	Without Constraint (By PSO)			With Constraint						
				By proposed iterative approach				By PSO		
	Size (kW)	P_{LOSS} (kW)	THD_{VM} (%)	Size (kW)	P_{LOSS} (kW)	THD_{VM} (%)	No. of HLF reqd.	Size (kW)	P_{LOSS} (kW)	THD_{VM} (%)
6	2409	104.5827	5.8645	2101	105.9474	4.9995	21	2101	105.9474	4.9995
7	2281	105.4532	8.2644	1488	115.7386	4.9981	26	1488	115.7386	4.9981
8	1953	109.6822	7.7735	1347	117.3346	4.9997	26	1347	117.3346	4.9997
9	1619	115.6814	8.5750	1032	125.4375	4.9939	27	1033	125.0019	4.9989
10	1402	119.3097	9.2732	841	130.7052	4.9937	25	841	130.7052	4.9937

11	1375	119.9341	9.2359	828	130.9617	4.9945	21	829	130.423	4.9989
12	1313	121.2299	9.0796	803	131.6298	4.9943	30	803	131.6298	4.9943
13	1131	125.8596	10.1975	631	138.3818	4.9937	29	632	138.1103	4.9990
14	1072	127.4696	11.1225	558	141.9798	4.9953	24	558	141.9798	4.9953
15	1014	129.8604	11.5057	514	144.6482	4.9950	33	514	144.6482	4.9950
16	949	132.9448	11.6992	475	147.3392	4.9928	33	477	146.9814	4.9995
17	846	138.2577	13.2653	No solution is obtained within the range of DG size considered						
18	795	141.1026	13.2933							
26	2280	106.2704	5.9627	1960	107.8782	4.9975	26	1960	107.8782	4.9975
27	2127	108.4085	6.1041	1793	110.3533	4.9998	27	1793	110.3533	4.9998
28	1725	113.3460	7.9822	1154	121.7332	4.9989	18	1154	121.7332	4.9989
29	1537	115.2980	9.1749	910	127.6726	4.9982	24	910	127.6726	4.9982
30	1435	116.9658	9.2441	843	129.4185	4.9978	30	843	129.4185	4.9978
31	1259	122.3639	10.4209	669	137.3578	4.9999	31	669	137.3578	4.9999
32	1207	124.4824	10.84199	620	140.1900	4.9999	25	620	140.1901	4.9999
33	1148	127.8420	11.5497	557	144.5629	4.9986	30	557	144.5629	4.9986

TABLE III(C): OPTIMUM DG SIZES FOR IEEE-33 BUS NETWORK UNDER LOADING CONDITION L3

Bus no.	Without Constraint (By PSO)			With Constraint						
				By proposed iterative approach				By PSO		
	Size (kW)	P_{LOSS} (kW)	THD_{VM} (%)	Size (kW)	P_{LOSS} (kW)	THD_{VM} (%)	No. of HLF reqd.	Size (kW)	P_{LOSS} (kW)	THD_{VM} (%)
6	2373	106.7161	7.3670	1574	116.0666	4.9976	20	1574	116.0666	4.9976
7	2247	107.5475	10.0667	1076	130.1442	4.9978	29	1076	130.1442	4.9978
8	1915	111.6440	9.5743	962	131.2345	4.9967	30	962	131.2345	4.9967
9	1594	117.4489	10.5768	719	139.4795	4.9994	30	719	139.4795	4.9994
10	1382	120.9574	11.4260	572	144.9516	4.9937	24	573	144.4652	4.9970
11	1348	121.5623	11.3391	562	145.1475	4.9938	27	562	145.1475	4.9938
12	1294	122.8170	11.2514	543	145.6674	4.9934	29	544	145.2147	4.99873
13	1109	127.2962	12.4630	416	152.2082	4.9894	33	418	151.7686	4.9996
14	1056	128.8524	13.5220	No solution is obtained within the range of DG size considered						
15	999	131.1680	13.9470							
16	933	134.1569	14.1451							
17	831	139.3029	15.7552							
18	784	142.0610	15.8546							
26	2242	108.3491	7.4539	1468	118.0414	4.9978	29	1468	118.041408	4.9978
27	2086	110.4180	7.6088	1335	120.7577	4.9966	29	1335	120.757653	4.9966
28	1700	115.1906	9.7339	837	134.5301	4.9969	15	837	134.530085	4.9969
29	1507	117.0742	10.9901	651	140.8690	4.9945	30	652	140.54693	4.9978
30	1415	118.6867	11.1340	602.	142.3729	4.9977	32	602.	142.372908	4.9977
31	1243	123.9081	12.4361	470	149.7735	4.9975	31	470	149.773461	4.9975
32	1189	125.9587	12.8557	434	152.2483	4.9954	30	434	152.248339	4.9954
33	1131	129.2125	13.5618	No solution is obtained within the range of DG size considered						

TABLE IV(A): OPTIMUM DG SIZES FOR IEEE-69 BUS NETWORK UNDER LOADING CONDITION L1

Bus no.	Without Constraint (By PSO)			With Constraint						
				By proposed iterative approach				By PSO		
	Size (kW)	P_{LOSS} (kW)	THD_{VM} (%)	Size (kW)	P_{LOSS} (kW)	THD_{VM} (%)	No. of HLF reqd.	Size (kW)	P_{LOSS} (kW)	THD_{VM} (%)
6	2852	193.8726	1.2325	2852	193.8726	1.2325	19	2852	193.8726	1.2325
8	2781	169.4420	2.5252	2781	169.4420	2.52525	22	2781	169.4420	2.5252
10	1809	176.3554	2.6958	1809	176.3554	2.6958	24	1809	176.3554	2.6958
12	1382	180.6105	2.8806	1382	180.6105	2.8806	16	1382	180.6105	2.8806
14	923	187.6570	3.1842	923	187.6570	3.1842	25	923	187.6570	3.1842
16	794	189.2072	3.4022	794	189.2072	3.4022	24	794	189.2072	3.4022
18	707	190.7073	3.2015	707	190.7073	3.2015	20	707	190.7073	3.2015
20	668	191.6074	3.2610	668	191.6074	3.2610	29	668	191.6074	3.2610
22	646	192.1452	3.3067	646	192.1452	3.3067	22	646	192.1452	3.3067
24	612	193.2739	3.3379	612	193.2739	3.3379	27	612	193.2739	3.3379
26	548	195.4557	3.3719	548	195.4557	3.3719	29	548	195.4557	3.3719
53	2609	164.0936	2.9518	2609	164.0936	2.9518	20	2609	164.0936	2.9518
55	2339	154.9131	3.7874	2339	154.9131	3.7874	13	2339	154.9131	3.7874
57	1934	120.4056	5.7576	1685	121.8596	4.9978	28	1685	121.8596	4.9978
59	1822	101.3197	6.7866	1352	108.2864	4.9977	28	1352	108.2864	4.9977
61	1740	88.2164	7.8247	1125	102.7478	4.9963	20	1125	102.7478	4.9963
63	1680	91.605	7.9776	1066	106.7626	4.9961	17	1066	106.7626	4.9961
65	1334	114.2822	8.7725	772	130.8202	4.9993	32	772	130.8202	4.9993
67	1545	180.6032	2.6792	1545	180.6032	2.6792	19	1545	180.6032	2.6792
69	1096	187.5292	2.8139	1096	187.5292	2.8139	25	1096	187.5292	2.8139

TABLE IV(B): OPTIMUM DG SIZES FOR IEEE-69 BUS NETWORK UNDER LOADING CONDITION L2

Bus no.	Without Constraint (By PSO)			With Constraint						
				By proposed iterative approach				By PSO		
	Size (kW)	P_{LOSS} (kW)	THD_{VM} z(%)	Size (kW)	P_{LOSS} (kW)	THD_{VM} (%)	No. of HLF reqd.	Size (kW)	P_{LOSS} (kW)	THD_{VM} (%)
6	2881	194.0517	1.721675	2881	194.0517	1.7217	21	2881	194.0517	1.7217
8	2809	169.1438	2.2423	2809	169.1438	2.2423	20	2809	169.1438	2.2423
10	1826	176.1526	2.3338	1826	176.1526	2.3338	22	1826	176.1526	2.3338
12	1396	180.4709	2.4655	1396	180.4709	2.4655	18	1396	180.4709	2.4655

14	932	187.6652	2.7041	932	187.6653	2.7041	25	932	187.6653	2.7041
16	802	189.2491	2.8861	802	189.2491	2.8861	22	802	189.2491	2.8861
18	715	190.7828	2.6762	715	190.7828	2.6762	18	715	190.7828	2.6762
20	677	191.7041	2.7372	677	191.7041	2.7372	26	677	191.7041	2.7372
22	653	192.2547	2.7690	653	192.2547	2.7690	24	653	192.2547	2.7690
24	618	193.4060	2.7936	618	193.4060	2.7936	29	618	193.4060	2.7936
26	554	195.6332	2.8283	554	195.63326	2.8283	21	554	195.6332	2.8283
53	2636	163.7087	2.6256	2636	163.7087	2.6256	18	2636	163.7087	2.6256
55	2362	154.3933	3.3779	2362	154.3933	3.3778	13	2362	154.3933	3.3778
57	1953	119.3647	5.1329	1908	119.4071	4.9979	26	1908	119.4071	4.9979
59	1835	99.9924	6.0323	1558	102.4282	4.9993	27	1558	102.4282	4.9993
61	1754	86.7120	6.9749	1313	94.0984	4.9958	30	1313	94.0984	4.9958
63	1692	90.1588	7.1155	1245	98.1598	4.9977	16	1245	98.1598	4.9977
65	1347	113.2044	7.9039	903	123.3154	4.9994	25	903	123.3154	4.9994
67	1560	180.4811	2.3025	1560	180.4811	2.3025	21	1560	180.4811	2.3025
69	1108	187.5333	2.3944	1108	187.5333	2.3944	25	1108	187.5333	2.3944

TABLE IV(C): OPTIMUM DG SIZES FOR IEEE-69 BUS NETWORK UNDER LOADING CONDITION L3

Bus no.	Without Constraint (By PSO)			With Constraint						
				By proposed iterative approach				By PSO		
	Size (kW)	P_{LOSS} (kW)	THD_{VM} z(%)	Size (kW)	P_{LOSS} (kW)	THD_{VM} (%)	No. of HLF reqd.	Size (kW)	P_{LOSS} (kW)	THD_{VM} (%)
6	2837	193.9901	1.4401	2837	193.9901	1.4401	18	2837	193.9901	1.4401
8	2757	169.8620	2.9071	2757	169.8620	2.9071	21	2757	169.8620	2.9071
10	1799	176.6575	2.9796	1799	176.6575	2.9796	23	1799	176.6575	2.9796
12	1376	180.8416	3.1754	1376	180.8416	3.1754	15	1376	180.8416	3.1754
14	915	187.8085	3.4849	915	187.8085	3.4849	27	915	187.8085	3.4849
16	790	189.3416	3.7233	790	189.3416	3.7233	25	790	189.3416	3.7233
18	704	190.8267	3.5298	704	190.8267	3.5298	27	704	190.8267	3.5298
20	665	191.7187	3.5922	665	191.7187	3.5922	27	665	191.7187	3.5922
22	643	192.2517	3.6381	643	192.2517	3.6381	21	643	192.2517	3.6381
24	609	193.3668	3.6683	609	193.3668	3.6683	26	609	193.3668	3.6683
26	545	195.5225	3.7005	545	195.5225	3.7004	28	545	195.5225	3.7005
53	2594	164.5909	3.4007	2594	164.5909	3.4007	21	2594	164.5909	3.4007
55	2326	155.5516	4.3459	2326	155.5516	4.3459	14	2326	155.5516	4.3459
57	1921	121.5426	6.4798	1451	126.7719	4.9983	29	1451	126.7719	4.9983
59	1809	102.7211	7.5430	1153	116.4710	4.9978	30	1153	116.4710	4.9978
61	1727	89.8117	8.6122	948	113.4924	4.9977	18	948	113.4924	4.9977
63	1669	93.1577	8.7754	897	117.3838	4.9953	21	897	117.3838	4.9953
65	1325	115.5293	9.5696	648	139.7973	4.9960	34	648	139.7973	4.9960
67	1537	180.8509	2.9219	1537	180.8509	2.9219	18	1537	180.8509	2.9219
69	1090	187.6815	3.0692	1090	187.6815	3.0692	24	1090	187.6815	3.0692

For the lateral, the unconstrained optimum size results in violation of the constraint for bus 57 to bus 65. In this case also, the results of the proposed method corroborate with those obtained from PSO. The results under loading condition L2 and L3 for IEEE-69 bus system are given in Table IV (B) and Table IV(C) respectively. The results shown in these Tables are now self-explanatory. From Table IV (A), Table IV (B) and Table IV(C) it can be seen that the maximum number of HLF required for this network is 34, whereas, minimum number of iterations required by PSO has been found to be 93 for bus 65 under loading condition L3. It means minimum number of HLF required by PSO in this problem is (93x10)=930. Thus, the results portrayed in Table III(A) to Table IV(C) present sufficient evidence that the number of HLF, and hence, the computation required by the suggested method is significantly less than that required by PSO. The reduction in power loss due to the resulting DG sizes is also clear from the Tables.

It is to be noted that the computational steps mentioned in section IV, in general, do not yield the DG sizes in integral values. To obtain the sizes in integral values, two additional HLF are to be executed for the nearest integral sizes on the two sides, lower and higher, of the size produced by the above computational steps. Among these two sizes, the one that results in lower loss with THD_{VM} remaining within limit, is chosen as the desired size. The number of HLF, shown for each bus in table III (A) to Table IV(C), has been counted including the two additional HLF. It may be further noted that, in reality, DGs are available in some standard sizes only. To obtain the desired standard size, the nearest standard sizes on the lower and higher side are to be considered instead of the nearest integral sizes. Between those two standard sizes, the one that produces lower amount of loss with THD_{VM} remaining within limit should be selected.

VI. CONCLUSION

This paper proposes a computationally efficient hybrid method for calculating the optimal size of inverter-based DG source placed at any selected location in a radial distribution network to minimize the network power loss in presence of limit on permissible harmonic distortion in bus voltages. The test results on IEEE-33 bus network and IEEE-69 bus network demonstrate the efficacy of the proposed methodology and show that the suggested approach can furnish the desired solution with significantly less computation compared to that required by PSO which is one of the most popular, efficient and widely used evolutionary computation based method. The suggested method can prove to be a very effective alternative to the evolutionary population based methods whenever any utility requires to find the optimal location and size for installation of an inverter-based DG unit in its distribution network. For such siting and sizing problem, the proposed algorithm is required to be repeated for all the potential candidate buses. Once the optimal DG sizes for all candidate buses are calculated, the optimal location and size for minimum network power loss is readily available from the list that can be prepared from the solutions for those buses. In that case, the total number of HLF required will be the summation of that required for each of those buses. However, the total number of HLF calculations required by PSO, in such cases, will also increase proportionally with the number of candidate buses. So, it is needless to mention that the amount of computation required by the proposed method will be significantly less than that required by PSO.

The method developed here is applicable for problems related to single DG placement. However, further study is required to extend the method for addressing the problem of simultaneous placement of multiple DGs. Investigation in that direction is being carried out by the present authors.

Appendix

A. Appendix – A

1) Determination of S_u and THD_u

Determination of these quantities will be necessary when any one from rule 1, rule 2, rule 4 and rule 6 is fired. The solution is achieved in two stages. In stage 1, the iterative method proposed in [24] is used for determination of an approximate estimate of S_u. The iterative steps required are briefly produced below:

$$S_u^{(r+1)} = \frac{S_u^{(r)} + S_u^{(old)}}{2}$$

where $r = 0,1,2,\ldots$ is the iteration number,

for $r = 0$, $S_u^{(old)} = S_{Min}$ if $S_u^{(r)} > S_u$

$= S_{Max}$ if $S_u^{(r)} < S_u$,

$$S_u^{(r)} = \frac{S_{Min} + S_{Max}}{2}$$

and, for $r > 0$, $S_u^{(old)} = S_u^{(r-1)}$ if $S_u^{(r)}$ and $S_u^{(r-1)}$ are on the two sides of S_u while $S_u^{(old)}$ remains unchanged when $S_u^{(r)}$ and $S_u^{(r-1)}$ are on the same side of S_u

The convergence criteria used is as follows:

If $P_{Loss}^{+} > P_{Loss}^{(r+1)} > P_{Loss}^{-}$, then $S_u^{(r+1)} > S_u$

If $P_{Loss}^{+} < P_{Loss}^{(r+1)} < P_{Loss}^{-}$, then $S_u^{(r+1)} < S_u$

If $P_{Loss}^{+} > P_{Loss}^{(r+1)} < P_{Loss}^{-}$, then $S_u^{(r+1)} \simeq S_u$

where, P_{Loss}^{+} and P_{Loss}^{-} are the losses obtained for DG size S^{+} and S^{-} respectively, $P_{Loss}^{(r+1)}$ is the loss calculated with DG size $S_u^{(r+1)}$, $S^{+} = S_u^{(r+1)} + \Delta S$, $S^{-} = S_u^{(r+1)} - \Delta S$, $\Delta S = 0.01 p_1 \times S_u^{(r+1)}$, $r = 0,1,2,\ldots$ and p_1 is the perturbation factor. The perturbation factor used in this stage is 5% $(p_1 = 5)$. As a result, the estimate of S_u obtained is approximately within $\pm$ 2.5% of its actual value. Let it be called S_{approx}. It is to be noted that at the start of iteration (i.e., *r=0*), the above convergence criteria is required to be applied once on $S_u^{(r)}$, to check whether $S_u^{(r)} > S_u$ or $S_u^{(r)} < S_u$ or $S_u^{(r)} = S_u$. If $S_u^{(r)} = S_u$, no further iteration will be required. For a more accurate solution for S_u, a second stage (stage 2) of iteration is suggested in this paper. In stage 2, the iteration starts with S_{approx} as the initial guess $S^{(0)}$ of S_u. The perturbation factor (p_2) used in this stage is 0.5% $(p_2 = 0.5)$. Thus S_u obtained from this stage is approximately within $\pm 0.25\%$ of its actual value. The iterative steps are as follows:

1. Set iteration count $r = 0$, $S^{(r)} = S_{approx}$ and $p_2 = 0.5$.
2. Apply the convergence criteria of stage 1 on $S^{(r)}$ with $\Delta S = 0.01 p_2 \times S^{(r)}$.
3. If $S^{(r)} < S_u$ set $S^{(r)} = S^{+}$, $m = 1$ and go to step 5, else go to next step.
4. If $S^{(r)} > S_u$ set $S^{(r)} = S^{-}$, $m = -1$ and go to next step, else go to step 9.
5. Set iteration count $r = 0$, $S^{(r)} = S_{approx}$ and $p_2 = 0.5$.
6. Apply the convergence criteria of stage 1 on $S^{(r)}$ with $\Delta S = 0.01 p_2 \times S^{(r)}$.
7. If $S^{(r)} < S_u$ set $S^{(r)} = S^{+}$, $m = 1$ and go to step 5, else go to next step.
8. If $S^{(r)} > S_u$ set $S^{(r)} = S^{-}$, $m = -1$ and go to next step, else go to step 9.
9. Set $S^{(old)} = S^{(r)}$.
10. $r = r + 1$.
11. $S^{(r)} = S^{(old)} + m \times \Delta S$.
12. If $P_{Loss}^{(r)} < P_{Loss}^{(r-1)}$, go to step 5, else go to step 10.
13. Set $S^{(old)} = S^{(r)}$.
14. Set $S_u = S^{(old)}$.
15. Print and/or display S_u.
16. End

In the above iterative steps, $S^{+} = S^{(r)} + \Delta S$ and $S^{-} = S^{(r)} + \Delta S$. $P_{Loss}^{(r)}$ and $P_{Loss}^{(r-1)}$ are losses for DG size $S^{(r)}$ and $S^{(r-1)}$ respectively. THD_u is obtained from the HLF results for the size S_u.

B. Appendix – B

1) Determination of THD_m

It is important to note that

1. Determination of THD_m is not necessary when anyone from rules (1) to (5) is fired. The necessary comparison of THD_{Min} with THD_m required for rule 3 can be achieved by comparing THD_{Min} with THD_{VM}^{+}, where, THD_{VM}^{+} is the value of THD_{VM} for DG size S_{Min}^{+}, and $S_{Min}^{+} = S_{Min} +$ (a small positive perturbation in DG size). If $THD_{VM}^{+} < THD_{Min}$, then $THD_m < THD_{Min}$ i.e., $THD_m < THD_L$, whereas, $THD_m = THD_{Min} = THD_L$ if $THD_{VM}^{+} > THD_{Min}$. Similarly the comparison between THD_{Max} and THD_m required for rule 5 can be done by comparing THD_{Max} with THD_{VM}^{-}, where, THD_{VM}^{-} is the value of THD_{VM} for DG size S_{Max}^{-}, and $S_{Max}^{-} = S_{Max} +$ (a small negative perturbation in DG size).

If $THD_{VM}^{-} < THD_{Max}$, $THD_m < THD_{Max}$ i.e., $THD_m < THD_L$, whereas, $THD_m = THD_{Max} = THD_L$ if $THD_{VM}^{-} > THD_{Max}$.

2. Determination of THD_m is required if rule 6 is fired. However, if $THD_m < THD_L$ then final determination of THD_m may not be necessary. In this case, if the value of THD_{VM} obtained at any step in the process of finding THD_m is found to be less than THD_L , it is then ensured that $THD_m < THD_L$, and the process is then stopped.
3. Determination of THD_m requires S_m to be determined. The nature of a *THD* curve has a similarity with that of a loss curve in the sense that both initially decreases with increase in DG size, and, after attaining a minimum, goes on increasing monotonically. Due to this similarity, S_m can be determined in the same manner as S_u is done, and hence, the same iterative scheme can be used with S_u replaced by S_m and P_{Loss} replaced by THD_{VM} . THD_m is obtained as a byproduct of this process without requiring any additional calculations.

C. Appendix – C

1) Determination of S_{L1} and S_{L2}

Determination of S_{L1} is necessary if rule 4 is fired whereas S_{L2} will have to be determined when rule 2 is fired. Both S_{L1} and S_{L2} will be required if rule 6 is fired provided it is identified that $THD_m < THD_L$. An iterative method is suggested that requires only a few HLF to find out S_{L1}. The method is explained with the help of Fig. C (a), where the first estimate $S_{L1}^{(1)}$ is obtained as the size corresponding to the point of intersection between the THD_L line and the line joining (S_{Min}, THD_{Min}) and $(S_{Max}, 0)$ using simple geometry as follows:

$$\frac{THD_L}{THD_{Min}} = \frac{S_{Max} - S_{L1}^{(1)}}{S_{Max} - S_{Min}} \tag{C.1}$$

$$S_{L1}^{(1)} = S_{Max} - \frac{THD_L}{THD_{Min}}(S_{Max} - S_{Min}) \tag{C.2}$$

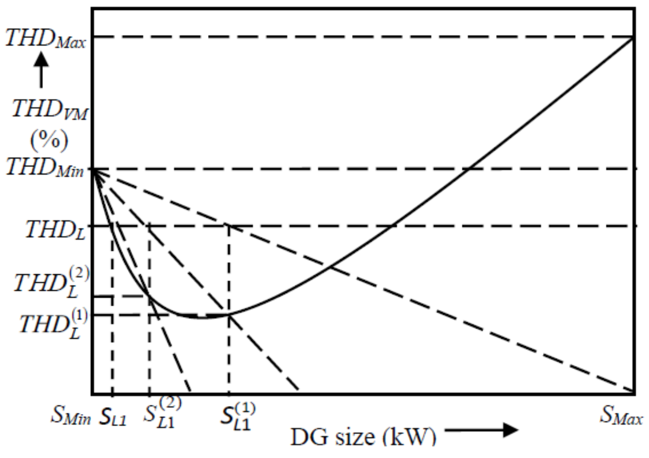

(a)

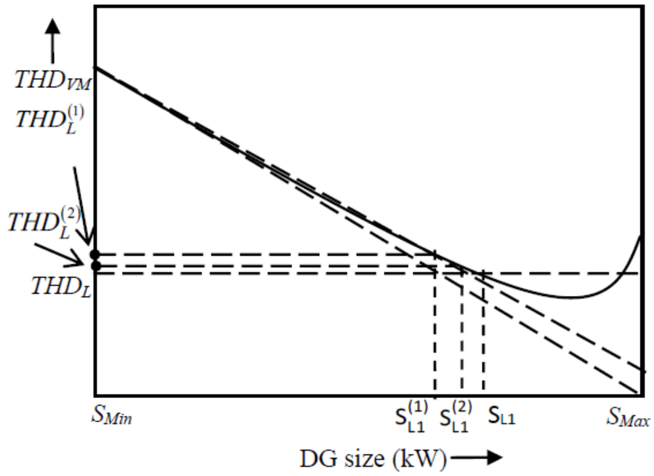

(b)

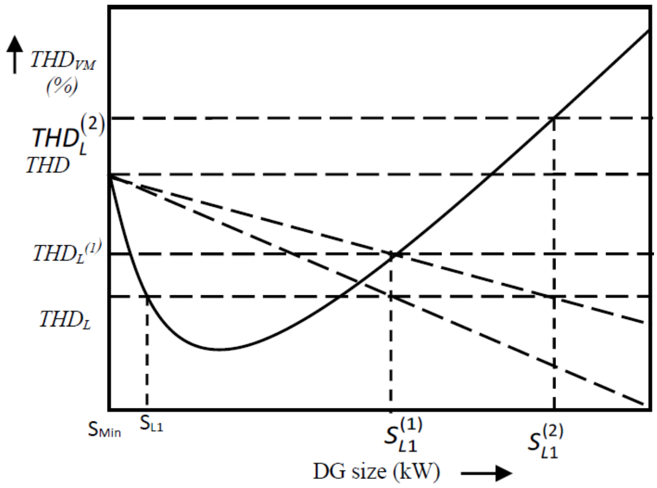

(c)

Fig. C. Demonstration of the iterative method for determination of S_{L1}. (a) Case I :when $S_{L1} < S_{L1}^{(1)} < S_{L2}$; (b) Case II :when $S_{L1} > S_{L1}^{(1)} < S_{L2}$; (c) Case III: when $S_{L1} < S_{L1}^{(1)} > S_{L2}$.

$THD_L^{(1)}$, the actual value of THD_{VM} on the *THD* curve at the size $S_{L1}^{(1)}$, is then obtained from HLF. A second estimate $S_{L1}^{(2)}$ is then obtained after joining the points (S_{Min}, THD_{Min}) and $(S_{L1}^{(1)}, THD_L^{(1)})$, and applying the same geometric approach as follows:

$$S_{L1}^{(2)} = S_{L1}^{(1)} - \frac{THD_L - THD_L^{(1)}}{THD_{Min} - THD_L^{(1)}}(S_{L1}^{(1)} - S_{Min}) \tag{C.3}$$

$THD_L^{(2)}$ corresponding to $S_{L1}^{(2)}$ is obtained from HLF. The iterative process continues with the iterative steps given by equation (C.4) until the estimated value of S_{L1} converges with the actual value as shown in Fig. C.

$$S_{L1}^{(r+1)} = S_{L1}^{(r)} - \frac{THD_L - THD_L^{(r)}}{THD_{Min} - THD_L^{(r)}}(S_{L1}^{(r)} - S_{Min}) \tag{C.4}$$

where, $r = 0,1,2,\ldots$ *r* is the number of iteration. For *r*=0, $S_{L1}^{(r)} = S_{Max}$, $THD_L^{(r)}=0$.

The convergence criterion is as follows:

$$\left|THD_L^{(r+1)} - THD_L\right| \le \sigma$$

where σ is the tolerance

It is to be noted that as the actual size S_{L1} is not known, the convergence is checked by the magnitude of the error between the values of THD_{VM} obtained for the estimated size and the actual value of THD_L. In the curve shown in Fig. C(a), $S_{L1} < S_{L1}^{(1)} < S_{L2}$, but there may be other situations where $S_{L1} > S_{L1}^{(1)} < S_{L2}$ (shown in Fig. C(b)) or $S_{L1} < S_{L1}^{(1)} > S_{L2}$ (shown in Fig. C(c)). In addition to these differences, each of the three situations has its distinguishing feature. In the first situation, $S_{L1}^{(2)}$ is always less than $S_{L1}^{(1)}$, whereas, in the second and third cases, $S_{L1}^{(2)}$ is always greater than $S_{L1}^{(1)}$. However, in the second case, $THD_L^{(2)}$ is always less than $THD_L^{(1)}$, but, $THD_L^{(2)}$ is always greater than $THD_L^{(1)}$ in the third situation. These features ensure an early detection (after second iteration only) of this difference between the two situations which is essential for proceeding with iterations. A minute observation of the figures, Fig. C(a), Fig. C(b) and Fig. C(c), can reveal that, in the first and second situations, the iteration will always lead to convergence, but, in the third case it will diverge. In fact, in the third case, $S_{L1}^{(r+1)} > S_{L1}^{(r)}$ for all $r > 0$. Once this diverging situation is detected after second iteration, the iterative process is repeatedly restarted with S_{Max}/n replaced by $S_{Max}/(n+1)$; $n = 1, 2, \ldots$ as the value of $S_{L1}^{(r)}$ for r=0, until diverging condition is avoided.

The same iterative approach is also used to determine S_{L2} with the first estimate $S_{L2}^{(1)}$ obtained as the size corresponding to the point of intersection between the THD_L line and the line joining (S_{Max}, THD_{Max}) and $(S_{Min}, 0)$. The final value of S_{L2} is obtained in the same manner as S_{L1} is obtained. In this case the three different situations are given by $S_{L1} < S_{L2}^{(1)} < S_{L2}$, $S_{L1} < S_{L2}^{(1)} > S_{L2}$, and $S_{L1} > S_{L2}^{(1)} < S_{L2}$. the third situation is a diverging one, and the iteration is required to be restarted repeatedly till diverging condition persists

D. Appendix – D

1) Harmonic data

TABLE D1: NON-LINEAR LOAD DATA (IN % OF NOMINAL BUS LOADING)

Loading condition	For IEEE-33 bus		For IEEE-69 bus	
L1	Bus No.	% non-linearity	Bus No.	% non-linearity
	6	10	8	12
	8	15	11	10
	11	10	17	10
	14	10	21	15
	20	12	49	20
	24	20	55	10
	28	15	61	10
	30	10	64	15
L2	10% non-linearity at all the buses		10% non-linearity at all the buses	
L3	No non-linear load present		No non-linear load present	

Nominal bus loadings are available in references [16] for IEEE-33 bus network and [17] for IEEE-69 bus network. Combination of six-pulse converter, twelve-pulse converter, arc furnace and fluorescent lamp has been used as nonlinear loads in this study. The harmonic spectrum of these harmonic loads, used for modelling them, are available in [23-25] and have been reproduced here in Table D2 for ready reference

TABLE D2: CURRENT HARMONIC SPECTRUM OF DIFFERENT TYPES OF LOAD

Harmonic order current	Magnitude in % of fundamental current			
	6-pulse Inverter	12-pulse Inverter	ASD	Fluorescent lamp
1	100	100	100	100
3	0	0	0	19.2
5	19.41	1.8	18.24	10.7
7	13.09	1.6	11.9	2.1
9	0	0	0	1.4
11	7.58	6.6	5.73	0.9
13	5.86	5.4	4.01	0.6
15	0	0	0	0.5
17	3.79	0.33	1.93	0

19	3.29	0.3	1.39	0
23	2.26	1.5	0.94	0
25	2.41	1.3	0.86	0
29	1.93	0.25	0.71	0
31	0	0	0.62	0
35	0	0.2	0.44	0
37	0	0.8	0.38	0
41	0	0.4	0	0

CONFLICT OF INTEREST

Barnali Motling, Subrata Paul and Sunita Haldar nee Dey declares that the submitted work was carried out without any conflict of interest. The authors therefore declares no conflict of interest.

AUTHOR CONTRIBUTIONS

Barnali Motling and Subrata Paul developed the methodologies for the analysis of IEEE 33 bus. Barnali Motling conducted the research, analyzed the data and also extended the study for IEEE 69 bus. Subrata Paul and Sunita Haldar nee Dey supervised the project. All authors had approved the final version, shaped the study, interpreted the results and drew conclusions to develop the suggested methodology along with the writing of final manuscript.

ACKNOWLEDGMENT

We would like to thank the Department of Electrical Engineering, Jadavpur University, Kolkata, India, for all the supports extended to us for carrying out the research work.

REFERENCES

[1] T. Ackermann, G. Anderson, and L. Soder, "Electricity market regulations and their impact on distributed generation," in *Proc. International Conference on Electric Utility Deregulation and Restructuring and Power Technologies*, pp. 608-613, April 2000.

[2] G. Pepermans, J. Driesen, D. Haeseldonckx *et al.* "Distributed generation: Definition, benefits and issues," *Centre for Economic Studies, Energy Transport & environment, Energy Policy*, vol. 36, no. 5, pp. 787-798, August 2003.

[3] "Modeling and simulation of the propagation of harmonics in electric power networks. I. Concepts, models, and simulation techniques," *IEEE Transactions on Power Delivery*, vol. 11, no. 1, pp. 452-465, Jan. 1996.

[4] J. Arrrilaga, D. A. Bradley, and P. S. Bodger, *Power System Harmonics*, John Wiley and Sons, New York, 1985.

[5] "Effects of harmonics on equipment," Report of the IEEE Task Force on Harmonic Impacts, *IEEE Trans*. on *Power Delivery*, vo1. 8, no.2, pp. 672-680, April 1993.

[6] A. F. A. Kadir, A. Mohamed, H. Shareef *et al.*, "Optimal placement and sizing of distributed generations in distribution systems for minimizing losses and THD_v using evolutionary programming," *Turkish Journal of Electrical Engineering & Computer Sciences*, pp. 2269-2282, 2013.

[7] A. A. Abdelsalam, A. A. Zidan, and E. F. El-Saadany, "Optimal DG allocation in radial distribution systems with high penetration of non-linear loads," *Electrical Power Comp. and Syst. Taylor & Francis*, vol. 43, pp. 1487–1497, 2015.

[8] S. Biswas, S. K. Goswami, and A. Chatterjee, "A study of the factors influencing the optimal size and site of distributed generations," *Journal of Clean Energy Technologies*, vol. 2, no. 1, pp. 28-33, January 2014.

[9] A. Parizad, A. H. Khazali, and M. Kalantar, "Sitting and sizing of distributed generation through Harmony Search Algorithm for improve voltage profile and reduction of THD and losses," in P*roc. IEEE Canadian Conf. Electrical and Computer Engineering*, pp. 1-7, May 2010.

[10] M. Q. Duong, T. D. Pham, T. T. Nguyen, A. T. Doan, and H. V. Tran, "Determination of optimal location and sizing of solar photovoltaic distribution generation units in radial distribution systems," *Energies*, vol. 12, p. 174, January 2019.

[11] O. Amanifar and M. E. H. Golshan, "Optimal distributed generation placement and sizing for loss and THD reduction and voltage profile improvement in distribution systems using particle swarm optimization and sensitivity analysis," *Int. Journal on Technical and Physical Problems of Engineering*, vol. 73, no. 2, pp. 47-53, June 2011.

[12] V. R. Pandi, H. H. Zeineldin, W. Xiao *et al.*, "Optimal penetration levels for inverter-based distributed generation considering harmonic limits," *Electrical Power Systems Research*, vol. 97, pp. 68-75, January 2013.

[13] V. R. Pandi, H. H. Zeineldin, and W. Xiao, "Determining optimal location and size of distributed generation resources considering harmonic and protection coordination limits," *IEEE Transactions on Power Syst*em, vol. 28, no. 2, pp. 1245-1254, May 2013.

[14] R. M. Sasiraja, K. Muthulakshmi, S. V. Kumar, and T. Abinaya, "PSO based optimal distributed generation placement and capacity by considering harmonic limits," *Tech. Gaz.*, vol. 24, pp. 391-398, 2017.

[15] B. Motling, S. Paul, and S. H. Nee Dey, "Siting and sizing of DG unit to Minimize loss in distribution network in the presence of DG generated harmonics," in *Proc. International Conference on Emerging Frontiers in Electrical and Electronic Technologies (ICEFEET)*, pp. 1-5, 2020.

[16] J. Teng and C. Chang, "Backward/forward sweep-based harmonic analysis method for distribution systems," *IEEE Transactions on Power Delivery*, vol. 22, pp. 1665–1672, 2007.

[17] C. Bud and B. Tomoiaga, "The load flow calculation in harmonic polluted radial electric networks with distributed generation," in *Proc. 9th Int. Conf. Electrical Power, Quality and Utilization*, 2007.

[18] I. Archundia-Aranda and R. O. Mota–Palomino, "Harmonic load flow method for radial distribution networks," in *Proc. 14th International conference on Harmonics and Quality of Power – ICHQP*, pp. 1-5, 2010.

[19] B. Motling, S. Paul, and S. H. N. Dey, "A novel iterative approach for optimal sizing of distributed generation units for loss minimization in distribution network," *International Journal of Industrial Electronics and Electrical Engineering (IJIEEE)*, vol. 5, no. 1, pp. 63-68, January 2017.

[20] J. Kennedy and R. Eberhart, "Particle swarm optimization," in *Proc. International Conference on Neural Networks*, vol. 4, pp. 1942-1948, 1995.

[21] S. Yarat, S. Senan, and Z. Orman, "A comparative study on PSO with other metaheuristic methods," in *International Series in Operations Research & Management Science,* B. A. Mercangöz, Ed., Applying Particle Swarm Optimization, Springer, pp. 49-72.

[22] M. E. Baran and F. F. Wu, "Network reconfiguration in distribution systems for loss reduction and load balancing," *IEEE Transactions on Power Delivery*, vol. 4, pp. 1401-1407, 1989.

[23] M. E. Baran and F. F. Wu, "Optimal capacitor placement on radial distribution systems," *IEEE Transactions on Power Delivery*, vol. 4, no. 1, January 1989.

[24] N. Acharya, P. Mahat, and N. Mithulananthan, "An analytical approach for DG allocation in primary distribution network," *Electrical Power & Energy Syst*em, vol. 28, no. 10, pp. 669-678, December 2006.

[25] Task Force on Harmonics Modelling and Simulation, "Modelling and simulation of the propagation of harmonics in electric power network part 11: sample systems and examples," *IEEE Transactions on Power Delivery*, vol. 11, no. 1, pp.466-474, January 1996.

[26] Task Force on Harmonics Modelling and Simulation, Transmission & Distribution Committee, "Test systems for harmonics modelling and simulation," *IEEE Power Engineering Society*.

[27] *IEEE Recommended Practice and Requirements for Harmonic Control in Electrical Power Systems*, IEEE Std. 519-1993, NY: IEEE.

Barnali Motling received her B.E. in electrical engineering, in 1992 from Shivaji University and M.E. in electrical power systems, in 2002 from Pune University, Maharashtra, India. She is currently pursuing her Ph.D. in (power systems) from Jadavpur University, Kolkata, India. Her areas of interest include micro grid, operation and planning of distribution system studies and impact of harmonic distortions on power systems.

Subrata Paul is associated with the Department of Electrical Engineering at Jadavpur University, Kolkata (West Bengal), India. He has published several research papers in international, national journals and conferences. His special field of interest includes micro grid, operation and planning of distribution system, optimization techniques, power quality, power system analysis, transient stability and FACTS applications.

.

Sunita Halder nee Dey received her B.E from Jalpaiguri Government College, and her M.E. and Ph.D from BESU, Kolkata Electrical Engineering, India in electrical engineering in 1998, 2001 and 2006 respectively. She is presently working with the Department of Electrical Engineering at Jadavpur University, Kolkata (west bengal), India. She has published several research papers in International and National Journals and Conferences. She has also co-authored a book on power system operation and control. Her special field of interest includes power system operation and control, micro grid, opf, voltage stability and facts applications